Modeling exponential decay in maximum capacitance across specified flight patterns in small aircraft

Pete B. Rigas[1], and Chetan S. Kulkarni[2],

[1] *Cornell University, Ithaca, NY, 14850, USA*
rigas.pete@gmail.com, pbr43@cornell.edu

[2] *KBR, Inc., NASA Ames Research Center, Moffett Field, CA, 94035, USA*
chetan.s.kulkarni@nasa.gov

ABSTRACT

With increased autonomy being integral part of unmanned aerial system (UAS), during the flight the vehicle needs to have accurate estimation of the state of health and its capabilities to perform and achieve mission success with out-most safety. Batteries are key of an electric-propulsion aircraft is its most pertinent resource. It is very important to know the state of charge of the batteries. In order to do estimate the state of charge the health state is key which is directly related to the flight profiles flown by the vehicle and its operational conditions.

In this work a methodology is presented to generate predictions for flight plans that experience anomalies, or unexpected mechanical failures in the engine due to a parasitic load in a specified stage of the flight that must return to its starting point of origin, we begin by describing the procedures by which a sequence of steps will be carried out to exponentially weigh the impact of different stages of a flight towards thermal strain on the capacitance $C_{\max}$ of the battery during each flight.

1. INTRODUCTION

Drawing from a previous 2014 work (Hogge & et. al, 2014) in which the authors sought to improve methods of generating flight predictions for small aircraft, the methodology and approach that follows will generate flights predictions of a similar type, for flights with individual stages of specified duration, so as to improve the maintenance of batteries and other equipment that are involved in the aircraft throughout flight. Moreover, to avoid having to perform laboratory tests on batteries after a fixed number of flights within a cycle, the model heavily relies on a free parameter choice to model the expected decay of the capacitance of the battery.

In contrast to the remaining flight time that is put forth in (Hogge & et. al, 2014), the approach is also aimed towards quantifying the exponential decay in the maximum capacitance, due to a parasitic load that is inserted within a fixed stage of the flight, and imposed for the remaining duration of the flight. To categorically separate and study the rate of change of exponential decay of the maximum capacitance of different batteries, parasitic loads of exponential, or of polynomial, magnitude are computed for consistent choices of β parameters. From the percentage of the maximum capacitance that the battery is observed to hold after a given cycle, the exponential factor that is temporally weighed in the duration of all stages of the flight allows for broader prognostics reflection, pertaining not only to equipment maintenance but also to total duration of a flight, and the accompanying SOC. Other works, including (Goebel & Eklund, 2007),(Kulkarni et al., 2010),(Kulkarni et al., 2011),(Sankararaman & Goebel, 2013a),(Sankararaman & Goebel, 2013b),(Saha, Saha, & Goebel, 2009) offer detailed discussions of either the experimental set up of tests which were used to test the accuracy of different numerical models, in addition to architectural schemes of offline battery maintenance, insofar as to further study capacitance degradation.

With example upper and lower bounds on the maximum capacitance decay for a wide variety of flights from different batteries in the publicly available HIRF repository (Kulkarni et al., 2015). The data set contains HIRF tests experiment data conducted on an electric fixed wind UAV Edge 540. The e-UAV is a 33% sub-scale version of the Zivko Aeronautics Inc. Edge 540 T tandem seat aerobatic aircraft. This vehicle has been actively used to facilitate the rapid deployment and evaluation of

remaining flying time prediction algorithms for electric aircraft(Hogge & et. al, 2014).

The parameter choice and resulting numerical behavior provides a formalism through which experiments consisting of flights with either longer duration, more complicated pattern with a larger number of stages, or varying electromagnetic radiation in the ambient environment of the flight, can be accounted for through adjustment of the β parameter, within the power of the exponent.

To characterize different flight plans from which sets of predictions will be generated, the approach detailed below will:

- provide calculations of the time duration of each segment of a flight, depending on the magnitude of the current exerted by the engine over each time interval, which will be determined by the current at the end of the flight that the engine asymptotically reaches in the final stages of each plan,
- introduce an exponentially decaying factor, whose magnitude is numerically determined by enforcing a summation, which is determined by a sequence of multiplicative, freely chosen parameters $\{\beta_i\}$, the minimum and maximum of which are not only chosen to be proportional to the duration of separate periods of the flight, but also to the magnitude of the change of current in each stage of the flight,
- computing the Fourier coefficients and series of current versus time plots from a prescribed set of flight plan data, from which predictions for upcoming, future flight plans will be generated by correlating, from the change in the magnitude of the exponential factor that is used to model the decay in the maximum capacitance of the circuit across multiple flights.

2. GENERAL APPROACH

In this section an overview of the developed approach is discussed. The Fourier series representation of each flight plan is obtained by approximating the temporal duration of each segment of an arbitrary flight plan through the individual steps which include:

- fixing a coordinate axis to measure applicable sine **or** cosine modes of the Fourier series representation which will be enforced after a smooth, polynomial approximation to the stage of the flight has been determined,
- computing a sufficient number of Fourier coefficients so that the corresponding Fourier series representation of the flight plan sufficiently represents all current measurements for each point in time of the real flight plan before introducing a Fourier series, obtainable through a suitable trigonometric basis$\{\sin(\frac{n\omega_0 t}{T}), \cos(\frac{n\omega_0 t}{T})\}_{n\in\mathbf{N}}$, where the normalizing period T used to compute the coefficient basis is the duration of the specified stage of the flight with n steps over which the smooth approximation is enforced, $T = \sum_{i=1}^{n} t_i$, which can be realized by ensuring that for all $t_i \in T$, given arbitrary flight segments $\mathcal{T}^{(i)}$,
- numerically determining a threshold of the Fourier modes $\mathcal{N}$ for which the mean squared error, for a generalized Fourier series $\sum_n a_n^2 + b_n^2$, or alternatively, $\sum_n a_n^2$ or $\sum_n b_n^2$, for Fourier cosine and sine series, respectively, beyond which the aforementioned summations does not substantially decrease, and hence, do not pose significant benefits towards generating more informative and reliable predictions.

Next, given such a Fourier series representation of the flight plan after a suitable polynomial approximation, in addition to the exponentially decaying factor for computing the change in the maximum and minimum capacitance that will be defined, the approach will generate predictions for flights plans of the following types, all of which are dependent on the duration of the specific stage of the flight, as well as the time stamp throughout the stage of the flight at which the plan is to be terminated.

- Flight Plan Type A: Given a set of experimental trials, it will be demonstrated how to compute an accompanying rate of exponential decay in the maximum capacitance over successive flights that is proportional to the magnitude, and duration, of the thermal stress and accordingly, the mechanical work, that is applied to the engine for each flight. From this factor, predictions will be readily generated for flights that are terminated in the beginning stages of a flight by:
  - computing the exponential decay of the maximum capacitance $C_{\max}$ across subsequent flights,
  - computing the **decrease** in $\mathcal{N}$ that is requisite to satisfy the piecewise conditions for R and f, which formally can be realized by incorporating, on average per segment of each flight, a specified number of Fourier modes in the series representation of the flight plan, which can be used to accommodate predictions for different time stamps throughout a fixed stage of a flight by continuously varying the rightmost endpoint in time on which the polynomial root finding method generates smooth approximations from the experimental current versus time data.

- Flight Plan Type B: Given a set of experimental trials, predictions for more complicated flight patterns can be generated by making use of the predictions generated for flights of the previously defined type, in the sense that a flight pattern of Type B can be analyzed, from predictions of fights of Type A by implementing:
    - a prescribed number Fourier modes $\mathcal{N}$ in the series approximation in the beginning phase of the flight during which a current is beginning to flow in the circuit of the engine, from which predictions of a termination of the flight plan in the next stage of the flight, hence the name Type B, can be generated implementing the change in maximum capacitance from the previous flight plan, in addition to the minimum and maximum rates of exponential decay in $C_{\max}$, granted that the smooth polynomial approximation not violate the piecewise condition that $|R(t_i) - f(t_i)| < \epsilon$ for all times t_i preceding the unforseen abortion of the flight in its earlier stage.
- Flight Plans Types C,D,E: Repeating the same observations and formulations for flight plants of Type A and Type B mutatis mutandis gives immediate generalizations of other flight plans for which the unforseen abortion of the flight can occur. In particular, flight plans of Type C, Type D, and Type E, respectively, describe excursions on which the same maximum capacitance value (which is the $C_{\max}$ value computed from previous flights in a given sequence, determined from an initial capacitance value in the first flight of the sequence which we set to be at the 100% threshold), the final time stamp t_f are which the flight is terminated.
- Flight Plan Type X; Pursuant of further generalizations, the preceding observations and formalism can be applied mutatis mutandis to new flights patterns, of emerging interest, for an arbitrary but countable number of intervals over which a flight can be terminated.

3. IMPLEMENTATION

To test the Fourier series implementation and exponentially decaying capacitance factor to calculate the change in $C_{\max}$ values across successive flights, given a set of training data through a given sequence of flights beforehand, the approach will be implemented by executing the following steps:

- Running an auxiliary algorithm in Matlab which will return the **approximate time intervals**, and respective duration's, of each stage of a given flight, which will be dealt with in two of the following cases:
    - **Case 1: (Flight plans in which the ending current reading for the final stage of the flight vertically asymptotes to values higher than those in preceding stages of the flight)** For flight plans of Case 1, one can easily generate time intervals for the intermediate stages of the flight plan by extending a horizontal line and linearly searching below such a threshold to obtain isolated segments of the flight during which polynomial approximations via the root finding method can be determined. From the current value that is exerted near the end of the flight from which the horizontal line is extended, a threshold δ will be chosen so that all current values below those of $\mathcal{H} - \delta$ will be returned.
    - **Case 2: (Flight plans in which the ending current reading for the final stage of the flight vertically asymptotes to values lower than those in the preceding stages of the flight)** For flight plans of Case 2, one can still generate analogous results corresponding to the time intervals for disjoint segments of a given flight plan, instead by enforcing that we lin-

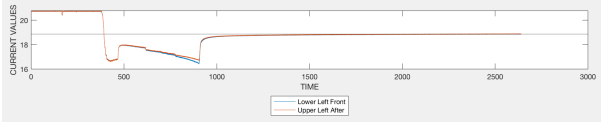

Figure 1. Example of Set 6, HIRF 77, plot of horizontal line for flight plan of Case 1

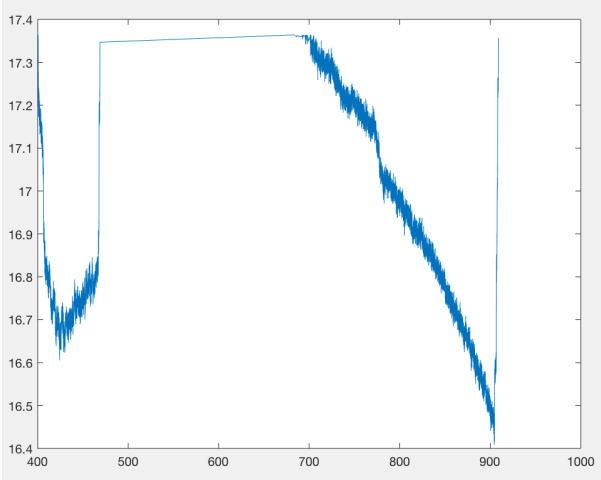

Figure 2. Plot of individual stages of the flight which are determined by linear inspection of the data through a specified threshold δ of the current asymptotic value given by the horizontal line at the end of the flight

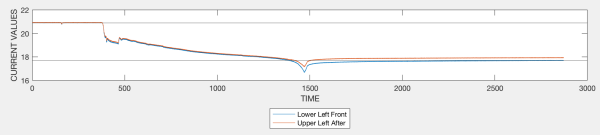

Figure 3. Example of Set 6, HIRF 80, plot of two horizontal lines for flight plan of Case 2

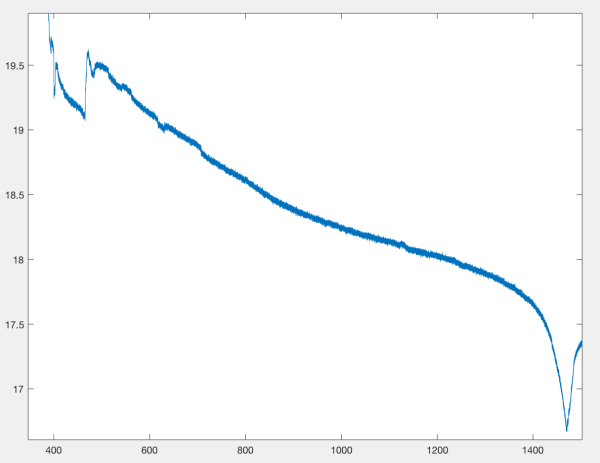

Figure 4. Plot of individual stages of the flight which are determined by linear inspection of the data through a specified threshold δ' of the current asymptotic value given by the horizontal line at the end of the flight

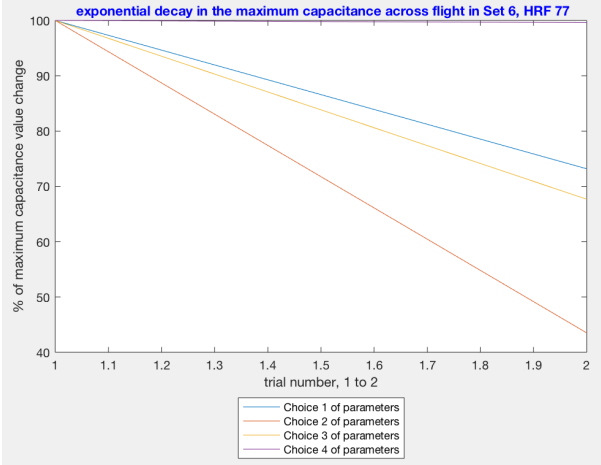

Figure 5. From the two demarcated stages of the flight given the return values of the auxiliary algorithm, the exponential decay in $C_{\max}$ is exhibited across each stage of the flight. Because the beginning and ending stages of the flight have been removed by the auxiliary algorithm to provide approximate time intervals from which thermal stress on the engine is exhibited, which in turn results in the expected strain on the capacitance. To illustrate the dependence of the $C_{\max}$ value that we report based on the choice of each β_i.

early search **above** the current value that the data asymptotically approaches at the final time stamp of the given flight, while simultaneously conditioning that the search also enforce the criterion that the isolated segments of the flight, of Case 2, not exceed the initial current starting value at the beginning of the flight. After executing such a search, the auxiliary algorithm will similarly return a set of times for each stage of the flight, from which exponentially decaying factors temporally weighed in each stage of the flight can be calculated.

- With the time durations of each stage, the values are fed into the exponentially decaying factor in time that measures the change in $C_{\max}$ value across subsequent flights, from which the number of modes $\mathcal{N}$ for each period of the flight will be determined, with an accompanying MSE. From the chosen flight examples above, we observe:
  - From Set 6, HIRF 77, disregarding the middle portion of the flight during which the magnitude of the current exerted on the current is approximately constant, one may compute the exponential decay in $C_{\max}$ by choosing suitable β_i, which in the case of this specific flight plan correspond to the real parameters that are linearly weighed in the temporal duration of all segments of the flight. With inspiration from exponential solutions to the one dimensional separable differential equation, we would expect that comparing the temporal durations of different stages of a flight, from the example in Set 6, HIRF 77 above, would yield an exponential decay $C_{\max}$, that would further reduce the change in capacitance on the second flight, as $C^{1\to 2}_{\max_1} \geq C^{1\to 2}_{\max_2} \Leftrightarrow |T^1_{6,77}| = |\{t_i \in T^1_{6,77}\}| \leq |T^2_{6,77}| = |\{t_j \in T^2_{6,77}\}|$, where $(C_{\max_2}, T^2)$ denote the capacitance and stage duration pair of a time deformation for the stage $T^1_{6,77}$ by linearly extending the duration of this stage of the flight forwards in time while maintaining an equal magnitude of current.
  - On the other hand, from Set 6, HIRF 80, the return values of time allow for calculations of the exponential decay in $C_{\max}$ for flights of Case 2. From noticeable differences in the trajectory of the flight from Set 6, the exponential decay in $C_{\max}$ is more sharp across the sequence of flights from that of HIRF 80.
- Finally, to establish sets of predictions for flight of varying types, namely flights that have previously defined histories each of which have been defined, a Fourier series expansion will be introduced by computing the accompanying coefficients.

case number	choice of parameters	$C_{\max}$ value on flight 2
1	$\beta_1 = \frac{1}{500}, \beta_2 = \frac{1}{5000}$	$C_{\max} \approx 0.73184 C_1$
2	$\beta_1 = \frac{1}{100}, \beta_2 = \frac{1}{5000}$,	$C_{\max} \approx 0.43509 C_1$,
3	$\beta_1 = \frac{1}{2500} = \beta_2$	$C_{\max} \approx 0.67686 C_1$
4	$\beta_1 = \frac{1}{25000}, \beta_2 = \frac{1}{25000}$	$C_{\max} \approx 0.99610 C_1$

Table 1. Table providing choice of parameters for each of the 4 cases in the plot.

case number	choice of parameters	$C_{\max}$ value after flight 2
1	$\beta_1 = \frac{1}{1000}, \beta_2 = \frac{1}{5000}$	$C_{\max} \approx 0.88692 C_1$
2	$\beta_1 = \frac{1}{200}, \beta_2 = \frac{1}{5000}$,	$C_{\max} \approx 0.644036 C_1$,
3	$\beta_1 = \frac{1}{300000}, \beta_2 = \frac{1}{50000}$	$C_{\max} \approx 0.995742 C_1$
4	$\beta_1 = \frac{1}{300} = \beta_2$	$C_{\max} \approx 0.99610 C_1$

Table 2. Table providing choice of parameters for each of the 4 cases in Figure 7.

3.1. Exponentially decaying capacitance

With the different choices of β parameters that will be further expounded upon in more sensitive calculations of the exponential decay in $C_{\max}$ that are inclusive of the beginning and ending periods of the flight, we will make the choice of free β parameters so that the decay of the maximum capacitance between neighboring flights reflects a rate of decay in the capacitance that is appropriate, in the sense that the rate of exponential decay does not fall into any one of the cases above in which the maximum capacitance in one flight from a previous one is almost left unchanged, at or around 99% of the previous $C_{\max}$, or at around 50% of the $C_{\max}$ for a typical flight.

4. WORKFLOW

Before proceeding with more details, the cartoon below provides a high level summary of each step in the approach.

- After obtaining flight plan data, we run the auxiliary algorithm which returns times of each stage of the flight, depending on the magnitude of the current at the beginning and ending stages of the flight,

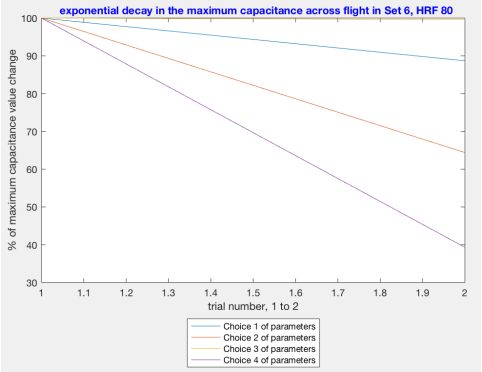

Figure 6. From the two demarcated stages of the flight given the return values of the auxiliary algorithm, the exponential decay in $C_{\max}$ is exhibited across different stages of this flight. Significantly, in comparison to the exponential decay that has been calculated from the previous flight of Case 1, we conclude that the $C_{\max}$, albeit decaying across both flights, decays more robust decay across the second flight because the temporal duration of the second stage of the flight, weighed by the multiplicative parameter β_2, is larger in magnitude in comparison to the β_2 parameter introduced for the second stage of the flight in Set 6, HIRF 77. As with the previous plot of the decay in $C_{\max}$, we introduce additional rates of exponential decay of $C_{\max}$, each of which are dependent on the specific choice of the β_i enforced throughout each stage of the flight.

- from which we enforce choices of free $\{\beta_i\}_{i \in \mathbf{N}}$ for calculating the exponential decay of $C_{\max}$.
- With lower and upper bounds on such a decay rate, we continue by introducing polynomials to smoothly approximate chamber data for current measurements in the aircraft engine, from which estimates of each stage of the flight are generated.
- To approximate flight plan data with a Fourier series, we proceed to make use of the smooth polynomial approximation to the flight data obtained in the previous step, as we compute the sine and cosine coefficients for the series expansion.
- As a result, we are able to generate sets of predictions for future flights, within the combinatorial space of all distinct outcomes, by computing the range of Fourier modes that can be used in the series to approximate the flight plan data, from which the MSE of the coefficients can be determined.
- Within the space of outcomes, we will introduce numerical bounds, based on the 30% SOC threshold, at which a flight can safely operate above the cutoff for a specified duration of time.

4.1. Fourier series approach

With a polynomial approximation obtained via the root finding method, given an arbitrary number of time

stamps before the flight plan is to be terminated, a modification to the usual Fourier sine and cosine coefficients will be introduced, in which each of the Fourier coefficients take the form,

$$a_n = \frac{1}{\sum_i t_i} \int_{\mathcal{T}_i} f(t) \cos\left(\frac{n\omega_0 t}{\mathcal{T}_i}\right) \mathrm{d}t \,,$$

and

$$b_n = \frac{1}{\sum_i t_i} \int_{\mathcal{T}_i} f(t) \sin\left(\frac{n\omega_0 t}{\mathcal{T}_i}\right) \mathrm{d}t \,,$$

where $\mathcal{T}$ denotes the stage of the flight over which the polynomial approximation has been obtained, and the normalizing constant for the period in the Fourier coefficients is the summation over all time stamps of the particular stage of the flight. As expected, f is smooth and from these expressions, one can obtain a series expansion of the form,

$$F(x) = \frac{a_0}{2} + \sum_{n, t \in \mathcal{T}_i} a_n \cos\left(\frac{n\omega_0 t}{\mathcal{T}_i}\right) + b_n \sin\left(\frac{n\omega_0 t}{\mathcal{T}_i}\right) ,$$

where each period $\mathcal{T}_i$ is not only dependent on the duration of the time interval of the stage of the flight, but also on the current of the magnitude $\mathcal{I}$ exerted on the engine given a flight trajectory. With such a Fourier series that one can obtained from the aforementioned trigonometric basis, introduced over each respective $\mathcal{T}_i$, one can generate flight predictions for flight plans of Type A, for arbitrary time stamps t_j before the initial stage of the flight, by first introducing a polynomial approximation of the flight data up to t_j, from which the MSE of all modes included in the expansion, $\sum_n a_n^2 + b_n^2$, is computed, with the truncation of the Fourier series taking the form,

$$F_{\mathcal{T}_i, t_i} = \frac{a_0}{2} + \sum_{n=1}^{\mathcal{M}_{t_i}} a_n \cos\left(\frac{n\omega_0 t}{\mathcal{T}_i}\right) + b_n \sin\left(\frac{n\omega_0 t}{\mathcal{T}_i}\right) ,$$

for a sufficient number of modes $\mathcal{M}_{t_j} < \mathcal{N}$. With a series approximation $F_{\mathcal{T}_i, t_i}$ above denoting the series truncation corresponding to the maximum time stamp $t_i < t_j$ for which the 30% SOC threshold can be maintained when the flight is terminated at the later time t_j, for all $t \in \mathcal{T}_i$.

To ensure that such a truncation adequately captures the degradation in $C_{\max}$ across successive trials, or potentially across trials with a particular battery of some type, an exponentially decaying, temporally dependent factor, iterative factor is defined, for time stamps $t_i, t_j \in \mathcal{T}_i$, and $t_i', t_j' \in \mathcal{T}_j$. Free parameters β_1, β_2, as demonstrated in plots for different decay rates of $C_{\max}$, multiplicatively accompany the time intervals $[t_i, t_f]$ and $[t_i', t_f']$, respectively over $\mathcal{T}_i$ and $\mathcal{T}_j$, during each of which a current of varying magnitude $\mathcal{I}$ is exerted. More generally, the power of the exponent is of the form $\sum_i \beta_i |\mathcal{T}_i|$, which takes into account for all stages, including the beginning and end of the flight, to be discussed in the **next** section for flights in Set 3.

For distinct time periods of each stage of the flight, the rates of exponential decay in $C_{\max}$, in addition to the series representation, together provide flight predictions by:

- computing the rate of exponential decay in the $C_{\max}$ across multiple flights with specified duration from the periods $\mathcal{T}_1^1, \cdots, \mathcal{T}_n^1, \cdots, \mathcal{T}_N^1, \cdots, \mathcal{T}_N^n$,
- incorporating the exponential decay mentioned in the previous step to determine the maximum durations of time for which the flight can maintain the 30% threshold, with the formula

$$\mathrm{SOC} = 1 - \frac{q_{\max} - q_b}{C_{\max}} \,,$$

  provided for computing the threshold in [2],
- and finally, determining the range of admissible Fourier modes in the series representation and computing the MSE for the number of modes.

4.2. Computation Case Studies

With a substantial array of Fourier coefficients, ranging from 200, $2,000$ to $10,000$, all of which together constituted a run time of approximately 3 days, numerical simulations were executed to determine properties relating to the convergence of Fourier series which can be obtained without having to resort to the computation of more than a few thousand Fourier series coefficients, up to different time stamps, one of which is at $t_f = 450$.

Beyond such numerical results, the plots below also demonstrate the distribution of higher frequency terms that could be used in the Fourier series expansion, where

number of Fourier modes	maximum Fourier mode	minimum Fourier mode
200	≈ 0.40793	$\approx 2.7658 \times 10^{-6}$
$2,000$	≈ 0.40793	$\approx 2.7049 \times 10^{-8}$
$10,000$	≈ 0.40793	$\approx 1.0955 \times 10^{-3}$

Table 3. Fourier cosine coefficients

number of Fourier modes	maximum Fourier mode	minimum Fourier mode
200	$\approx -8.6023 \times 10^{-4}$	≈ -21.1558
$2,000$	$\approx -8.6023 \times 10^{-5}$	≈ -21.1558
$10,000$	$\approx -1.7205 \times 10^{-5}$	≈ -21.1558

Table 4. Fourier sine coefficients

the computations of the Fourier coefficients are carried out for $10,000$ Fourier sine and cosine coefficients. Due to the significantly higher MSE associated with the Fourier sine coefficients for this example flight, we will only make use of the cosine coefficients in the expansion, from which the series expansion will be plotted for all 4938 time stamps of the flight.

4.3. Adjusting the free parameters in the exponentially decaying factor

From the description and implementation of the auxiliary algorithm as a proxy for the change in $C_{\max}$ across a single flight, from the given fixed ordering of the time stamps and the current measurements as the flight progresses, the assignment $\Phi : \mathbf{R}^+ \longrightarrow \mathbf{R}^+ : |t_j - t_k| \mapsto \beta_i$, for $j \neq k$, and $\beta_i > 0$, obtains a monotonic pairing of the time intervals of each stage of the flight with the freely chosen β_i, so that, throughout the variable duration of a given flight pattern:

- periods of shorter duration, in which the magnitude of the current $\mathcal{I}$ abruptly changes, are multiplicatively weighed more unfavorably in the discharge of capacitance of the circuit in the engine, while
- periods of longer duration, in which the current of magnitude $\mathcal{I}$ changes more gradually over the course of a stage in the flight, are multiplicatively weighed more favorably in terms of the impact on the maximum capacitance that the circuit can hold, and therefore, less adversely impact the circuit.

number of Fourier modes	MSE
200	$\approx 0.192276077317043$
$10,000$	$\approx 0.192276132208228$

Table 5. MSE values

number of Fourier modes	maximum Fourier mode	minimum Fourier mode
200	≈ 0.3139	$\approx 7.928 \times 10^{-6}$
$2,000$	≈ 0.3139	$\approx 7.857 \times 10^{-8}$

Table 6. Fourier cosine coefficients

number of Fourier modes	maximum Fourier mode	minimum Fourier mode
200	≈ 21.124	$\approx 2.466 \times 10^{-3}$
$2,000$	≈ 21.236	$\approx 2.466 \times 10^{-4}$

Table 7. Fourier sine coefficients

With such a convention of the free parameter assignment in hand, a range of exponentially decaying factors, and hence, of the maximum discharge of capacitance in the circuit, predictions can be realized. By means of providing examples of flight patterns for which the time intervals of each stage will be collected, from which the temporally adjusted weighted exponential decrease of the battery will be computed, consider the following sequence of flights from the publicly available NASA prognostic repository $\#15$.

5. PROCEDURE FOR GENERATING THE COMBINATORIAL SPACE OF FLIGHT PREDICTIONS

To produce effective, and informative, flight predictions given a numerically specified exponential rate of decay in $C_{\max}$, we will proceed with the following steps:

- Step 1 (**identifying the stage of the flight during which the prediction is to be established**): To systematically address all stages and times during which an anomaly could occur, whether through the flight plan or through a parasitic load of the circuit which grows exponential or polynomially with re-

number of Fourier modes	MSE
200	≈ 560.79416
$2,000$	≈ 561.902567337
$10,000$	≈ 5.62001093

Table 8. MSE values

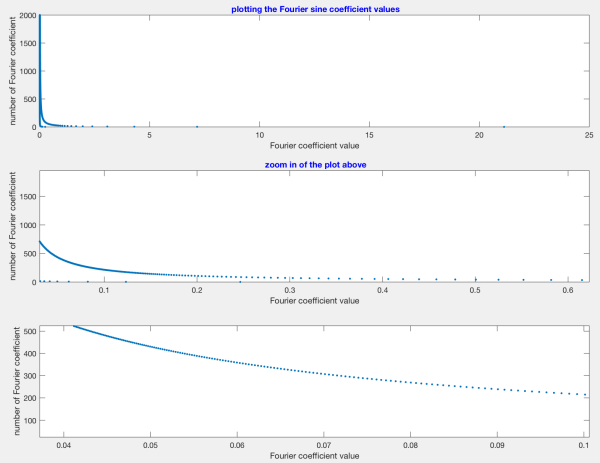

Figure 7. In contrast to similar plots of the Fourier cosine coefficients, the sine coefficients, for the truncated polynomial approximation up to the time stamp 450 before the current change occurs results in coefficients that are of opposite sine than those previously presented in the previous diagram. Although the coefficients in the first plot are qualitatively similar to those given in the previous diagram, they are of the opposite sign which nevertheless result in the same MSE. In the second and third plots, we observe the same quantitative behavior in the magnitude of the Fourier coefficients computed for a given frequency.

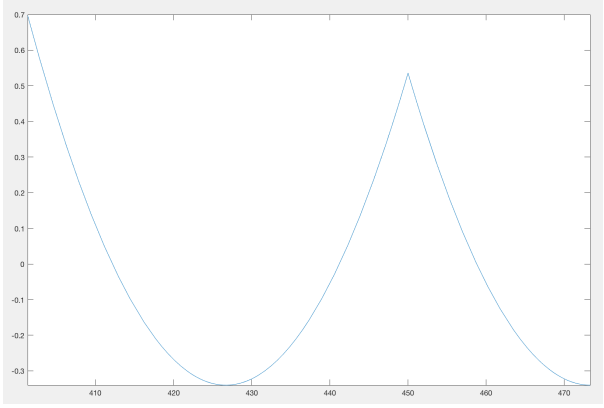

Figure 8. To more closely analyze the behavior of the series approximation from which predictions will be generated with a specified, attributable MSE, the behavior of the series approximation, as t varies linearly with respect to the time stamp which is incremented by a unit for each successive time stamp along the array, is depicted above.

spect to time which will be distinguished in future steps, we will introduce arbitrary time stamps $t^{(i)}_{\text{abort}}$ corresponding to each stamp $T^{(i)}$ of a given flight. From such time stamps in future flight plans that we designate as attributable to anomalies in the flight plan, predictions for the flight in question will be generated by:

- linearly varying the stamp $t^{(i)}_{\text{abort}}$ forwards in time for all admissible times in the stage $\mathcal{T}^{(i)}$ of the flight,
- combinatorially incorporating the minimum and maximum rates of exponential decay in $C_{\max}$ of the circuit, by means of introducing a suitable range of free parameters β_i in the exponentially decaying factor, insofar as to not only simulate varying rates of exponential decrease in the ability of the circuit to transport current, but to also account for flight plan anomalies in **each** stage of the flight,
- enforcing predictions for whether the flight should be terminated, by determining at which time stamp $t^{(i)}_{\text{SOC}} < t^{(i)}_{\text{abort}}$ the flight should be terminated, in order for the flight to maintain the 30% state of charge threshold given in [2].

- Step 2 (**computing informative ranges of the exponential decay of** $C_{\max}$): In order to pursue realistic predictions, we must also introduce upper and lower bounds for the exponential decay in $C_{\max}$. Pursuant of this goal, we wish to measure the change in exponential decay that we can attribute to a different choice of parameter β_j, say β'_j, satisfying $|\beta_j - \beta'_j| < \epsilon$ for arbitrary ϵ. Under these assumptions, the exponential factor for measuring the change in capacitance takes the form,

$$\overbrace{e^{\sum_{i\cap j}\beta_i\left(t^{(i)}_{\text{final}}-t^{(i)}_{\text{initial}}\right)+\beta_j\left(t^{(j)}_{\text{final}}-t^{(j)}_{\text{initial}}\right)}}^{\text{for first choice of }\beta_j} - \overbrace{e^{\sum_{i\cap j}\beta_i\left(t^{(i)}_{\text{final}}-t^{(i)}_{\text{initial}}\right)+\beta'_j\left(t^{(j)}_{\text{final}}-t^{(j)}_{\text{initial}}\right)}}^{\text{for second choice of }\beta_j},$$

where the real parameters β_j, β'_j are chosen during the stage $T^{(j)}$ of the flight, which has time duration $t^{(j)}_{\text{final}} - t^{(j)}_{\text{initial}}$. Because all of the remaining β_i, for $i \neq j$, are left fixed, enforcing a different choice of the β_j parameter amounts to a multiplicative, exponentially decaying factor, of the form,

$$e^{\sum_{i\cap j}\beta_i\left(t^{(i)}_{\text{final}}-t^{(i)}_{\text{initial}}\right)}\left(e^{\left(\beta_j-\beta'_j\right)\left(t^{(i)}_{\text{final}}-t^{(i)}_{\text{initial}}\right)}\right),$$

which illustrates how the exponential decay of $C_{\max}$ is dependent on the weight of each β_i, which is tuned for each $\mathcal{T}^{(i)}$. Additionally, to make even

more explicit the dependence of time, we will designate the arbitrary time stamps $t^{(i)}_{\text{abort}}$ as the times during each stage $\mathcal{T}^{(i)}$ during which the flight could be terminated, and more precisely, the time stamp in this stage of the flight during which the flight will exactly satisfy the SOC threshold that will be discussed at further length.

- Step 3 (**choosing flight data from the prognostics repository to compute exponential rates of decay in $C_{\max}$, from which bounds on the $C_{\max}$ will be obtained**: With remarks concerning how one would expect the $C_{\max}$ of the circuit to change across successive flights from the choice of each β_i, as a consequence it is important to designate the sets of experimental data from which exponential rates of decay in $C_{\max}$ will be computed.
- Step 4 (**beyond choosing the flight data: generalizing sets of predictions in flight plan abnormalities given a time stamp of flight termination**): With upper and lower bounds for $C_{\max}$ in hand, generating flight predictions now amounts to:
  - Implementing the user-defined time during which an arbitrary flight plan is to be aborted, due to either flight plan abnormalities or mechanical failures associated with the circuit, namely by choosing each possible stage of the future flight plans at which the anomaly could occur, and even more so, by accompanying rates of decay in the maximum capacitance,
  - generalizing the notion of abortions of a flight due to unforseen changes in the $C_{\max}$ value of the circuit, with the addition of another exponentially decaying factor appended to the exponential factor has has already been given and discussed, which is of the form,

$$\mathcal{C}^{\text{PL},T^{(i)}}_{\max_{i+1}} = \left(e^{\sum_i -\beta_i |t^{(i)}_{\text{initial}} - t^{(i)}_{\text{final}}|} \times e^{\beta^{\text{PL},\mathcal{T}^{(i)}}_{\mathcal{T}^{(i)}_{\text{PL}}} |t^{PL}_{\text{final}} - t^{PL}_{\text{initial}}|}\right) C_{\max_i} \, ,$$

which denotes the local exponential decay of $C_{\max}$ given a temporally dependent, exponentially increasing, parasitic load PL. Numerically, it is important to remark upon the nature of this exponential appendant, in the sense that the power of the exponential that is added onto the exponential can either be equal, less than, or greater in magnitude than the summation in the power of the first exponential that is dependent on both the β_i and duration of each stage $\mathcal{T}^{(i)}$ of the flight. One may also define the decay of the local capacitance due to a polynomial factor, instead of an exponential one, which is of the form,

$$\mathcal{C}^{\text{PL},T^{(i)}}_{\max_{i+1}} = \left(e^{\sum_i -\beta_i |t^{(i)}_{\text{initial}} - t^{(i)}_{\text{final}}|} \times \left(1 + (\beta^{\text{PL},\mathcal{T}^{(i)}}_{\mathcal{T}^{(i)}_{\text{PL}}} |t^{PL}_{\text{final}} - t^{PL}_{\text{initial}}|) t^{PL}_{\text{final}} + \frac{((\beta^{\text{PL},\mathcal{T}^{(i)}}_{\mathcal{T}^{(i)}_{\text{PL}}} |t^{PL}_{\text{final}} - t^{PL}_{\text{initial}}| t^{PL}_{\text{final}})^2}{2} + \cdots\right)\right) C_{\max_i} \, ,$$

for a parasitic load, polynomially increasing, which impairs the $C_{\max}$ value of the circuit, injected upon the circuit in stage $\mathcal{T}^{(i)}$ of the flight with corresponding choice of free parameters.

- Step 5 (**SOC formulas based on maximum capacitance formalism for the regular and local cases**): From expressions of $C_{\max}$ and $\mathcal{C}^{PL}$, we can make use of the formula for computing the SOC to propose 3 different formulas that can be used to compute the corresponding state of charge, each of which are of the form,

$$\text{SOC}_1 = 1 - \frac{q_{\max} - q_b}{e^{\sum_i -\beta_i \times t^{(i)}_{\text{initial}} - t^{(i)}_{\text{final}}} C_{\max}} \, ,$$

$$\text{SOC}_2 = 1 - (q_{\max} - q_b)/[e^{\sum_i -\beta_i |t^{(i)}_{\text{initial}} - t^{(i)}_{\text{final}}|} \times e^{\beta^{\text{PL},\mathcal{T}^{(i)}}_{\mathcal{T}^{(i)}_{\text{PL}}} |t^{PL}_{\text{final}} - t^{PL}_{\text{initial}}|} C_{\max}]$$

$$\text{SOC}_3 = 1 - (q_{\max} - q_b)/[1 + (\beta^{\text{PL},\mathcal{T}^{(i)}}_{\mathcal{T}^{(i)}_{\text{PL}}} |t^{PL}_{\text{final}} - t^{PL}_{\text{initial}}| t^{PL}_{\text{final}} + \frac{1}{2}(\beta^{\text{PL},\mathcal{T}^{(i)}}_{\mathcal{T}^{(i)}_{\text{PL}}} |t^{PL}_{\text{final}} - t^{PL}_{\text{initial}}| t^{PL}_{\text{final}})^2 + \cdots) C_{\max}] \, ,$$

respectively, each of which correspond to the SOC for the first formula for the capacitance introduced the earliest in the report, while the remaining 2 formulas below the first SOC equation denote expressions for the SOC due to the local capacitance $\mathcal{C}$ of the parasitic load, with either exponential rate of decay, or exponential-polynomial rate of decay.

- Step 6 (**summarizing the procedure: backtracking from t_{abort} to determine the intervals of time for which the current satisfies**

30% **SOC**): From either a flight or parasitically driven mechanical abnormality, we can make flight predictions by following the previously mentioned steps, in which exponentially weighing the duration of each flight, as mechanical or thermal stress on the engine, provides convenient interpretations for the total duration of a flight before falling before the SOC threshold.

5.1. Rate of decay of the local capacitance due to a parasitic load

As suggested through computations in previous tables, we are able to readily generate predictions for upcoming flights by specifying the stage of the flight at which the load is imposed, from which computations of the local capacitance, due to either polynomial or exponential decay, will be calculated. Thus, from such a rate of decay, it is possible to establish suggestions for the maximum flight time given the duration of each stage of the flight. Conversely, past flight data from previous mechanical malfunctions could also be interpreted, with the following approach. If the duration for either a mechanical malfunction or flight anomaly is known in a flight, an implementation the magnitude of the parasitic load, whether polynomial or exponential, can be computed by working backwards from the expressions given in the previous section. Namely, if the distance over which the mechanical or flight plan anomaly is known through experimentally gathered current measurements, then the distance over which the anomaly has occurred can be used to approximate the magnitude of the parasitic load responsible for the anomaly.

Furthermore, because an exponentially varying parasitic load that increases with time can be Taylor expanded into a polynomial of fixed degree, backwards calculations from the distance over which a flight anomaly have occurred could also be implemented to obtain a polynomial expression for the parasitic load that is responsible for the anomaly, whatever its type may be. In either circumstance, the approach fits within experimental data that is to be gathered, or has been gathered, to inform maintenance for future flights. Clearly, if the magnitude due to the parasitic load is sufficiently dominant, in the sense that the degradation due to the load prevents the flight from completing individual stages of a flight that are of the same duration from flights that it has already completed previously in a given sequence, then the flight should be terminated.

6. CONCLUDING REMARKS

By introducing an exponentially decaying factor that is temporally weighed in specific sets of current versus time measurements that are experimentally recorded for different flights, we are able to generate widely accommodating flight predictions that take into account the specific nature of the data, in this case the current that is supplied to the electric power-train throughout the flight, which is variable and can most certainly degrade with repeated use. In future work, we are continuing to pursue our interest of being able to continue generating sufficiently large combinatorial spaces from the Φ assignment. Furthermore, although the mapping is defined so that we do not assign multiple β free parameters to the $C_{\max}$ decay for time periods of a flight that are not equal, there are countably many mappings that we can construct to further experiment with the steepness of the $C_{\max}$ decay which could be of additional interest for aircraft's that are either built according to different specifications than the one in which HIRF chamber experiments were held. Certainly, the methodology and the approach presented here is able to address such changes in machinery by being able to explore families of Φ mappings, namely a function space of mappings $\Phi_{\mathcal{S}}$, where $\mathcal{S}$ is the sample space of times during individual stages of the flight. With a more general notion of the rate of change of the maximum capacitance with respect to not only the flight number of a cycle but also to the hardware specific requirements of the battery and equipment that are being used.

Another area of interest for future work includes being able to develop more specifications for other data structures that could arise in the experimentally gathered current readings in the truncated plots that are returned by the auxiliary algorithm as given in the appendix. With more complicated experiments and specifications either to the amount of current that will be delivered during a flight, or even on the duration of the flight itself, it would be helpful to continue expanding on the approach to make it more versatile to handle flights with an arbitrary number of stages, which could improve battery maintenance, as well as overall construction of the aircraft, for optimal aerodynamic performance in a wide variety of flight profile patterns. Although the estimates for the decay in the maximum capacitance will not be subject to electromagnetic radiation effects that are present in the background of the environment which can have a significant impact on the temperature at which the equipment operates, another exponential factor with its own free parameter accounting for the difference between the ambient temperature of the environment, and the maximum temperature at which the battery will continue to carry sufficient enough current above the SOC threshold, can be implemented.

REFERENCES

Goebel, K., & Eklund, N. (2007). Prognostic fusion for uncertainty reduction. In *Aiaa infotech@aerospace 2007 conference and exhibit.*

Hogge, E., & et. al. (2014). Verification of a remaining flying time predictions system for small electric aircraft. In *Annual conference of the phm society.*

Kulkarni, C., Biswas, G., Celaya, J. R., & Goebel, K. (2011). Prognostics techniques for capacitor degradation and health monitoring. In *The maintenance and reliability conference, marcon.*

Kulkarni, C., Biswas, G., Koutsoukos, X., Goebel, K., & Celaya, J. (2010). Physics of failure models for capacitor degradation in dc-dc converters. In *The maintenance reliability conference, marcon 2010 the maintenance reliability conference, marcon 2010.*

Kulkarni, C., Hogge, E., Quach, C., & Goebel, K. (2015). "hirf battery data set",. In *Nasa ames prognostics data repository.* NASA.

Saha, B., Saha, S., & Goebel, K. (2009). A distributed prognostic health management architecture. In *Ieee aerospace conference.*

Sankararaman, S., & Goebel, K. (2013a). Remaining useful life estimation in prognosis: An uncertainty propagation problem. In *Aiaa infotech conference.*

Sankararaman, S., & Goebel, K. (2013b). Uncertainty quantification in remaining useful life of aerospace components using state space models and inverse form. In *54th aiaa/asme/asce/ahs/asc structures, structural dynamics, and materials conference.*